

# A Remarkable *cis*- and *trans*-Spanning Dibenzylidene Acetone Diphosphine Chelating Ligand (dbaphos)

Amanda G. Jarvis,<sup>[a]</sup> Petr E. Sehnal,<sup>[a]</sup> Somia E. Bajwa,<sup>[a]</sup> Adrian C. Whitwood,<sup>[a]</sup> Xiangbiao Zhang,<sup>[b]</sup> Man Sing Cheung,<sup>[b]</sup> Zhenyang Lin,<sup>\*,[b]</sup> and Ian J. S. Fairlamb<sup>\*,[a]</sup>

*Dedicated to Professor Piet W. N. M. van Leeuwen for his distinguished contributions to the design of wide-angle spanning ligands*

**Abstract:** A multidentate and flexible diolefin–diphosphine ligand, based on the dibenzylidene acetone core, namely dbaphos (**1**), is reported herein. The ligand adopts an array of different geometries at Pt, Pd and Rh. At Pt<sup>II</sup> the dbaphos ligand forms *cis*- and *trans*-diphosphine complexes and can be defined as a wide-angle spanning ligand. <sup>1</sup>H NMR spectroscopic analysis shows that the β-hydrogen of one olefin moiety interacts with the Pt<sup>II</sup> centre (an anagostic interaction), which is supported by DFT calculations. At Pd<sup>0</sup>

and Rh<sup>I</sup>, the dbaphos ligand exhibits both olefin and phosphine interactions with the metal centres. The Pd<sup>0</sup> complex of dbaphos is dinuclear, with bridging diphosphines. The complex exhibits the coordination of one olefin moiety, which is in dynamic exchange (intramolecular) with the other “free”

olefin. The Pd<sup>0</sup> complex of dbaphos reacts with iodobenzene to afford *trans*-[Pd<sup>II</sup>(dbaphos)I(Ph)]. In the case of Rh<sup>I</sup>, dbaphos coordinates to form a structure in which the phosphine and olefin moieties occupy both axial and equatorial sites, which stands in contrast to a related bidentate olefin, phosphine ligand (“Lei” ligand), in which the olefins occupy the equatorial sites and phosphines the axial sites, exclusively.

**Keywords:** bite angle • coordination modes • density functional calculations • ligands effects • structure elucidation

## Introduction

Dibenzylidene acetone (dba-H) is an electron-deficient 1,4-diene ligand that coordinates transition metals in a variety of modes, through either the olefin as a 1,4-diene or bridging ligand, and/or carbonyl moieties, for example in [Rh(η<sup>5</sup>-C<sub>5</sub>Me<sub>5</sub>)(η<sup>2</sup>,η<sup>2</sup>-dba-H)]<sup>[1]</sup> and [Fe(CO)<sub>3</sub>(η<sup>4</sup>-(CO)(CH=CH Ph)<sub>2</sub>)]<sup>[2]</sup> in addition to other complexes (Fe,<sup>[3]</sup> Ru,<sup>[4]</sup> U<sup>[5]</sup> complexes; selected examples are given in Figure 1).<sup>[6]</sup> [Pd<sup>0</sup><sub>2</sub>-(dba-H)<sub>3</sub>] is the best known transition-metal complex<sup>[7]</sup> bearing a dba-H ligand, and is a widely used Pd<sup>0</sup> precursor in synthetic chemistry, catalysis and organometallic chemistry. Related complexes, [Pd<sup>0</sup><sub>2</sub>(dba-Z)<sub>3</sub>] and [Pd<sup>0</sup>(dba-Z)<sub>2</sub>] (dba-Z = dibenzylidene acetone with different Z-substituents),

have been reported.<sup>[8]</sup> In these complexes, intramolecular dba-H olefin–olefin exchange occurs readily at Pd<sup>0</sup>, through C=O coordination, with several conformers being accessible.<sup>[9]</sup> Addition of ligands (L) such as phosphines (monodentate or bidentate) or bipyridyls<sup>[10]</sup> give complexes of the type [Pd<sup>0</sup>(η<sup>2</sup>-dba)(L)<sub>2</sub>]. The platinum variant, [Pt<sup>0</sup><sub>2</sub>(dba-H)<sub>3</sub>], is also known.<sup>[11]</sup>

Recently, we reported a multidentate ligand based on the dba core structure, namely dbathiophos (an olefin–phosphine sulfide hybrid ligand),<sup>[12]</sup> which has a high affinity for cationic and neutral Cu<sup>I</sup> ions (see Figure 1); the Cu<sup>I</sup> complexes are competent catalysts for olefin cyclopropanation. Lei and co-workers reported that the chalcone-phosphino ligand (“Lei ligand”) effectively promotes Pd-catalysed Negishi cross-couplings.<sup>[13]</sup> This, coupled with other known positive dba effects in catalysis,<sup>[14]</sup> has encouraged us to explore new dba ligands containing a phosphine donor group(s).

Our efforts to synthesise a new phosphine ligand, dbaphos (**1**), and the eclectic array of Pt, Pd and Rh complexes that are accessible through complexation, are described herein. We envisaged that **1** could act as both a wide-angle spanning chelating and bridging ligand, indeed the ability of ligands to access both *cis*- and *trans*-geometries is of considerable interest.<sup>[15]</sup>

[a] Dr. A. G. Jarvis, Dr. P. E. Sehnal, Dr. S. E. Bajwa, Dr. A. C. Whitwood, Prof. Dr. I. J. S. Fairlamb  
Department of Chemistry, University of York  
York, YO10 5DD (UK)  
Fax: (+44) 1904-322516  
E-mail: ian.fairlamb@york.ac.uk

[b] Dr. X. Zhang, M. S. Cheung, Prof. Dr. Z. Lin  
Department of Chemistry, The Hong Kong University of Science and Technology, Clear Water Bay, Kowloon  
Hong Kong (P. R. China)  
E-mail: chzlin@ust.hk

Supporting information for this article is available on the WWW under <http://dx.doi.org/10.1002/chem.201203691>.

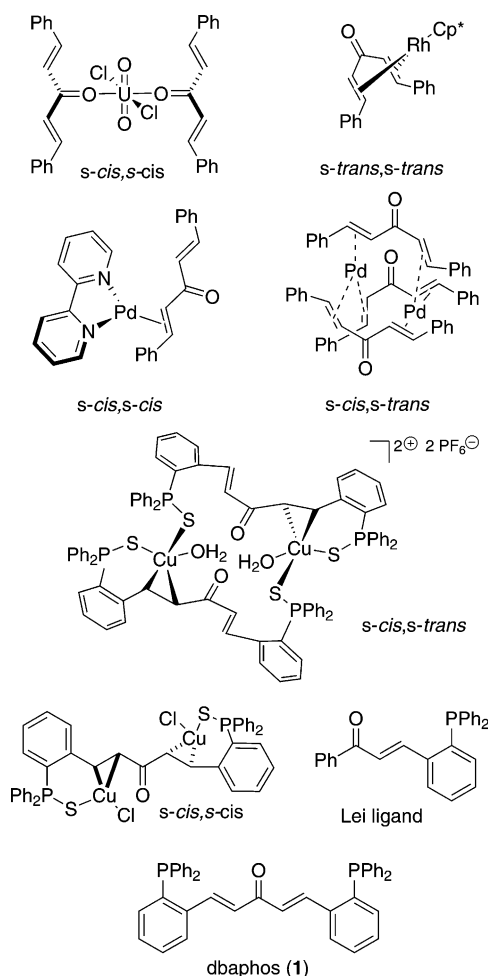
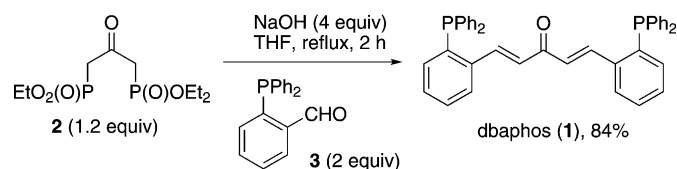


Figure 1. Representative dba-metal complexes, the “Lei” ligand and “dbaphos” ligand **1** (for the metal complexes the 1,4-dien-3-one conformations are denoted in the figure).

## Results and Discussion

Dbaphos **1** can in principle be prepared by Claisen–Schmidt condensation, Horner–Wadsworth–Emmons (HWE), or Wittig reactions. Having assessed all of these synthetic methods, the HWE reaction was found most acquiescent. For example, HWE reaction of bisphosphonate **2** (see the Supporting Information for preparative details) with *o*-diphenylphosphinobenzaldehyde (**3**) in the presence of NaOH at reflux for 2 h under inert atmosphere, affords dbaphos (**1**) (Scheme 1) in 84% yield (>96% purity, as determined by  $^{31}\text{P}$  NMR spectroscopy).<sup>[16]</sup> Crystals of **1**, suitable for X-ray diffraction analysis, were obtained by crystallisation from MeCN at  $-20^\circ\text{C}$  (Figure 2). The 1,4-dien-3-one

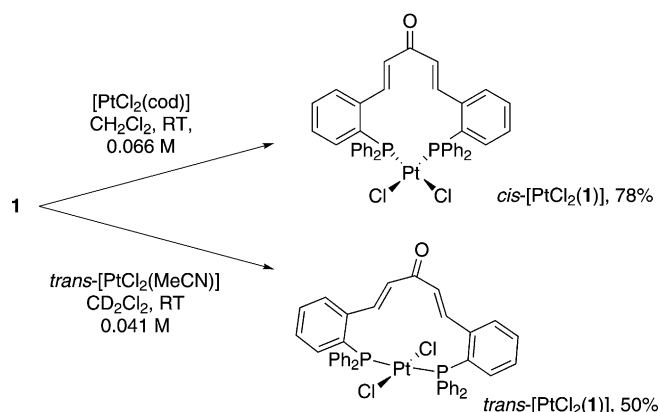


Scheme 1. Synthesis of dbaphos (**1**).

backbone exists in an extended linear *s-cis,s-cis* conformation. Changes in conformation about the 1,4-dien-3-one moiety, especially in solution, are expected (vide infra).

Ligand **1** has several potential coordination sites (i.e., phosphorus, olefin and carbonyl). Olefins are often considered as hemilabile moieties compared to phosphines, although the extent of hemilability depends on the metal centre.<sup>[17]</sup> In exploratory  $\text{Pt}^{\text{II}}$  complexation experiments separate equimolar reactions were carried out. Both *cis*- $[\text{PtCl}_2(\text{cod})]$  and *trans*- $[\text{PtCl}_2(\text{MeCN})_2]$  reacted with **1** in  $\text{CH}_2\text{Cl}_2$  to afford two isomeric  $[\text{PtCl}_2(\mathbf{1})]$  complexes (Scheme 2).

Our first reactions of *cis*- $[\text{PtCl}_2(\text{cod})]$  gave an insoluble material, which was most likely polymeric; on reducing the reaction concentration to 0.066 M a product soluble in  $\text{CH}_2\text{Cl}_2$  was formed. A single signal in the  $^{31}\text{P}$  NMR spectrum ( $\delta = 4.72$  ppm) indicated that the two phosphorus centres were in the same chemical environment, that is, the



Scheme 2. Synthesis of *cis*- $[\text{Pt}^{\text{II}}\text{Cl}_2(\mathbf{1})]$  and *trans*- $[\text{Pt}^{\text{II}}\text{Cl}_2(\mathbf{1})]$ .

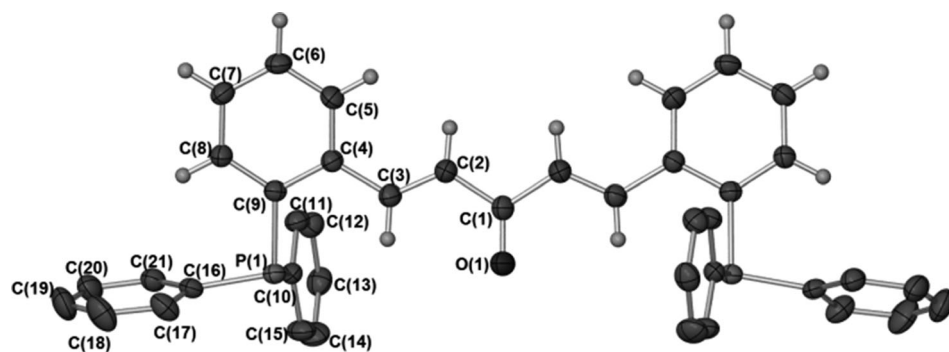


Figure 2. X-ray structure of dbaphos (**1**). Thermal ellipsoids shown at 50% probability; selected hydrogens omitted for clarity.

ligand acts as a symmetrical bidentate phosphine ligand. In  $\text{CD}_2\text{Cl}_2$ , the  $^1J_{\text{Pt,P}}$  coupling constant of the product derived from  $\text{cis}[\text{PtCl}_2(\text{cod})]$  and **1** is 3562 Hz, indicating that the phosphines are located *cis* to each other (at  $\text{Pt}^{\text{II}}$ ).<sup>[18a]</sup> The X-ray crystal structure of  $\text{cis}[\text{PtCl}_2(\mathbf{1})]$  supports the NMR spectroscopic evidence (Figure 3).

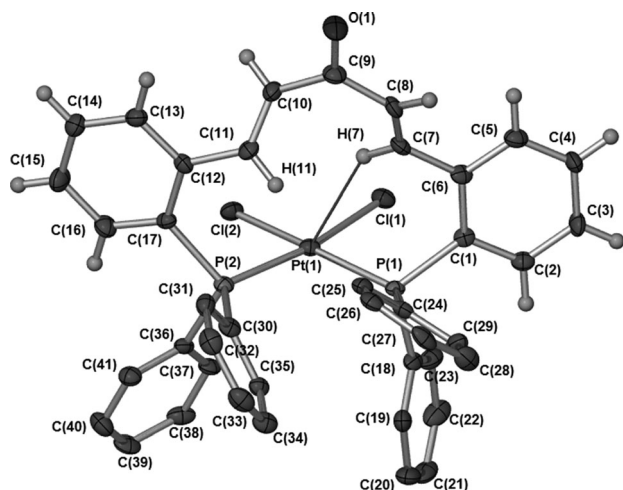


Figure 3. X-ray crystal structure of  $\text{cis}[\text{PtCl}_2(\mathbf{1})]$ . Selected hydrogen atoms removed for clarity. Thermal ellipsoids shown at 50%. Selected angles ( $^\circ$ ) include:  $\text{P}(2)\text{--Pt}(1)\text{--P}(1) = 105.89(5)$ ,  $\text{P}(2)\text{--Pt}(1)\text{--Cl}(2) = 81.18(5)$ ,  $\text{P}(1)\text{--Pt}(1)\text{--Cl}(2) = 169.71(4)$ ,  $\text{P}(2)\text{--Pt}(1)\text{--Cl}(1) = 167.60(4)$ ,  $\text{P}(1)\text{--Pt}(1)\text{--Cl}(1) = 86.49(5)$ ,  $\text{Cl}(2)\text{--Pt}(1)\text{--Cl}(1) = 86.45(5)$ .

The P–Pt–P bite angle in  $\text{cis}[\text{PtCl}_2(\mathbf{1})]$  is  $105.9^\circ$ , and is similar in size to other wide-bite-angle ligands such as Xantphos and related ligands.<sup>[18b,c]</sup> A comparison of the bite angles of Xantphos and dbaphos **1** shows that the latter has the larger bite angle by  $5^\circ$  (at  $\text{Pt}^{\text{II}}$ ). The X-ray crystal structure of  $\text{cis}[\text{PtCl}_2(\mathbf{1})]$  shows that the dbaphos ligand is not symmetrical around the  $\text{Pt}^{\text{II}}$  centre as shown by the difference of  $0.0268(19)$  Å in the two P–Pt bond lengths.

The P–Pt bonds are similar to related complexes with long P–Pt bonds (a search of the Cambridge structural database reveals that the mean P–Pt distance in *cis* complexes is 2.233 Å). One of the olefins (C(7)–C(8)) displays a short Pt–H contact, 2.642 Å.  $^1\text{H}$  NMR spectroscopic analysis shows that there is a  $\text{Pt}\cdots\text{H}$  interaction; the most electron-deficient olefin protons (H(7) and H(11) in the crystal structure) have shifted to  $\delta = 9.82$  ppm (+1.52 ppm) compared with the free ligand **1**. A rapid exchange process is occurring in solution, as indicated by the sharp olefin-proton signals.

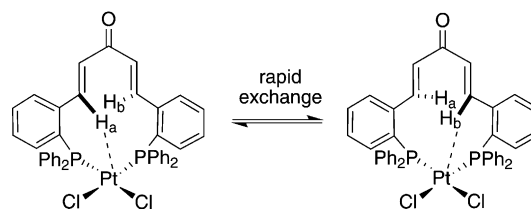
We have also evaluated the reactions of  $[\text{PdCl}_2(\text{cod})]$  with **1** (see Supporting Information). A *trans*- $[\text{PdCl}_2(\mathbf{1})]$  complex appears to have been formed with a solid-state  $^{31}\text{P}$  NMR spectrum showing a slightly distorted AB multiplet with a  $^2J_{\text{PP}}$  coupling of 540 Hz, indicative of *trans*-phosphines. Also, the most deshielded olefin protons share a chemical shift similar to the equivalent protons in *trans*- $[\text{PtCl}_2(\mathbf{1})]$ , being substantially different to *cis*- $[\text{PtCl}_2(\mathbf{1})]$ . However, we cannot

rule out the formation of dinuclear species and note limited product solubility in  $\text{CH}_2\text{Cl}_2$  and DMSO.

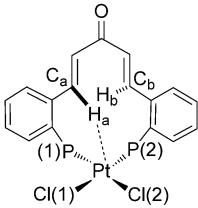
**On the interaction of the  $\beta$ -olefin hydrogen with  $\text{Pt}^{\text{II}}$ :** Interactions between N–H and C–H bonds and transition metals are well recognised.<sup>[19]</sup> Two different types of interactions have been clearly identified, namely agostic and anagostic interactions.<sup>[20]</sup> Agostic interactions refer to 3-centre-2-electron interactions and are characterised by small  $\text{M}\cdots\text{H}$  distances (ca. 1.8–2.3 Å), small C–H–M angles (ca.  $90\text{--}140^\circ$ ), and an upfield shift in  $\delta_{\text{H}}$  of the C–H upon coordination, along with low  $^1J_{\text{C,H}}$  values. Agostic interactions require the metal centre to be coordinately unsaturated, with an empty orbital available for  $\sigma$ -donation from the C–H bond. The term “anagostic” was used by Lippard and co-workers to describe any  $\text{C–H}\cdots\text{M}$  interactions that were not agostic.<sup>[21]</sup> Other terms such as “pregostic” have been used, and anagostic interactions also cover those described by hydrogen bonding. Anagostic interactions are characterised by larger  $\text{M}\cdots\text{H}$  distances (ca. 2.3–2.9 Å), larger C–H–M angles (ca.  $110\text{--}170^\circ$ ) and by a downfield shift in  $\delta_{\text{H}}$  of the C–H upon coordination (a general feature of hydrogen bonds). Anagostic interactions do not need an empty orbital and therefore can involve 18-electron metal centres. For  $d^8$  square-planar complexes either agostic or anagostic interactions are able to occur. While the  $\text{N–H}\cdots\text{M}(d^8)$  interactions can be confidently described with a 3-centre-4-electron bond (hydrogen bond), the  $\text{C–H}\cdots\text{M}(d^8)$  interactions are believed to be much more complicated. It has been proposed that a weak hydrogen bond is involved.<sup>[19a]</sup>

The X-ray diffraction data for  $\text{cis}[\text{PtCl}_2(\mathbf{1})]$  shows a Pt–H interaction of 2.642 Å in the crystal structure, and a downfield shift of the H(7) and H(11) protons in the  $^1\text{H}$  NMR spectrum, suggesting an anagostic interaction of some type is present. Using theoretical calculations we wished to gain a greater understanding of this interesting interaction. It was also clear from the  $^1\text{H}$  NMR spectrum that exchange of the H(7) and H(11) protons (see Figure 3) was rapid, as the spectrum was sharp, with only one signal observed for these protons. DFT calculations were performed with no simplification of  $\text{cis}[\text{PtCl}_2(\mathbf{1})]$ , to gain an insight into the nature of the short platinum-proton interaction and the exchange process shown in Scheme 3 (H(7) and H(11) are denoted  $\text{H}_a$  and  $\text{H}_b$ ).

DFT calculations at the MPW1PW91 level were carried out for complex optimisation (details given in the Supporting Information).<sup>[22]</sup> The structure of  $\text{cis}[\text{PtCl}_2(\mathbf{1})]$  was optimised, with the calculated structural values agreeing with



Scheme 3. Rapid exchange of  $\text{Pt}\cdots\text{H}_{a/b}$ .

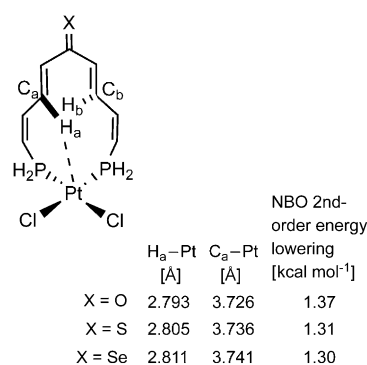
Table 1. Comparison of experimental and calculated bond lengths [Å] in *cis*-[PtCl<sub>2</sub>(**1**)].


Bond	Experimental	Calculated	Difference
Pt–H <sub>a</sub>	2.642	2.595	0.047
Pt–C <sub>a</sub>	3.450	3.422	0.028
Pt–C <sub>b</sub>	3.480	3.455	0.025
Pt–P(1)	2.2802(13)	2.304	–0.0238
Pt–P(2)	2.2534(14)	2.297	–0.0436
Pt–Cl(1)	2.3592(13)	2.376	–0.0268
Pt–Cl(2)	2.3395(12)	2.371	–0.0415

those obtained by experiment (Table 1). The largest deviation was seen between the calculated and experimental C–H<sub>a</sub>...Pt distances. This could be expected as the hydrogen atoms in the experimental structure were placed using a “riding model”. As the calculated C<sub>a</sub>...Pt and C<sub>b</sub>...Pt distances were in good agreement with the experiment it is believed that the calculated C–H...Pt is more realistic than the experimental value. The barrier for the exchange was calculated to be 1.04 kcal mol<sup>–1</sup> in electronic energy and 1.16 kcal mol<sup>–1</sup> in free energy, which is consistent with the experimental observation that the exchange is very rapid. It is also consistent with a previously reported theoretical estimate of a C–H...Pd<sup>II</sup> interaction of 0.8 kcal mol<sup>–1</sup>.<sup>[23]</sup>

In order to understand the nature of the C–H...Pt interactions, natural bond orbital (NBO) analyses<sup>[24]</sup> were carried out on the basis of the electronic structures calculated for *cis*-[PtCl<sub>2</sub>(**1**)]. No appreciable Wiberg bond index<sup>[25]</sup> (a measure of bond strength) was seen for the close C–H...Pt contact. However, an appreciable second-order perturbation energy related to the donor–acceptor interaction of Pt–(d<sub>z</sub><sup>2</sup>)→C<sub>a</sub>–H<sub>a</sub>(σ\*) was found (in which *z* is the axis perpendicular to the square plane of the complex studied)<sup>[24]</sup>. This second-order energy lowering was calculated to be 1.59 kcal mol<sup>–1</sup>, which points to the involvement of a weak hydrogen bond. The second-order energy lowering is a measure of the donor–acceptor interaction.<sup>[24]</sup> To further support the notion of a weak hydrogen bond, the C–H...Pt contact distances for the simplified model complexes shown in Figure 4 were calculated and the relevant NBO analysis performed. The results indicate that the less electronegative X is (X = O, S and Se), the longer the C–H...Pt contacts are and a smaller second-order energy lowering is observed. The changes along the series of different X atoms are only marginal, suggesting that the C–H...Pt interactions are weak.

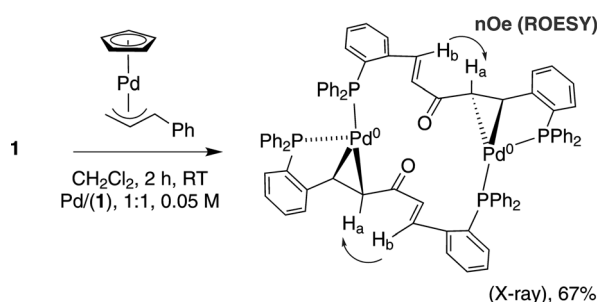
The results from the NBO analysis are consistent with both the small energies calculated from DFT for the exchange and with the experimental observations. A deshielded proton resonance for H<sub>a</sub>/H<sub>b</sub> is seen in the <sup>1</sup>H NMR spectrum of *cis*-[PtCl<sub>2</sub>(**1**)] with respect to the free ligand. In light

Figure 4. NBO results for a simplified model of *cis*-[PtCl<sub>2</sub>(**1**)].

of the calculations, the deshielding effect in *cis*-[PtCl<sub>2</sub>(**1**)] can be attributed to a weak hydrogen bond resulting from the Pt(d<sub>z</sub><sup>2</sup>)→C<sub>a</sub>–H<sub>a</sub>(σ\*) interaction.

Interestingly, dissolution of *cis*-[PtCl<sub>2</sub>(**1**)] in [D<sub>6</sub>]DMSO leads to isomerisation<sup>[26]</sup> to *trans*-[PtCl<sub>2</sub>(**1**)] with a *J*<sub>Pt,P</sub> value of 2565 Hz. Heating *cis*-[PtCl<sub>2</sub>(**1**)] to 60 °C for 4 h results in complete isomerisation to *trans*-[PtCl<sub>2</sub>(**1**)]. The latter complex can also be directly synthesised from *trans*-[PtCl<sub>2</sub>(MeCN)<sub>2</sub>] to give a product in 50 % yield; the complex in CD<sub>2</sub>Cl<sub>2</sub> exhibits a <sup>31</sup>P chemical shift of δ = 14.9 ppm and <sup>1</sup>*J*<sub>Pt,P</sub> coupling constant of 2577 Hz, indicating the phosphines are *trans*-disposed. The <sup>1</sup>H NMR spectrum of *trans*-[PtCl<sub>2</sub>(**1**)] shows that the 1,4-dien-3-one is symmetrical and most likely in a *s-trans,s-trans* conformation. An insoluble precipitate (including reactions in [D<sub>6</sub>]DMSO) is observed within hours, which we believe is a binuclear Pt<sup>II</sup> complex or higher order polymer containing **1**. DFT calculations show that the difference in energy between *cis*- and *trans*-[PtCl<sub>2</sub>(**1**)] complexes (on the complete structures of *cis*- and *trans*-[PtCl<sub>2</sub>(**1**)] complexes) is significantly different, with the *trans*-geometry being more thermodynamically stable (Pt, Δ*G*<sup>0</sup> = –8.0 kcal mol<sup>–1</sup>), which confirms its feasibility as an isomeric product.

**Synthesis of Pd and Rh complexes containing dbaphos:** We next examined the synthesis of Pd<sup>0</sup> and Pd<sup>II</sup> complexes containing ligand **1**. Experiments involving reaction of [Pd<sup>0</sup><sub>2</sub>-(dba-H)<sub>3</sub>] with **1** led to mixtures of products (see Supporting Information), therefore we turned to [Pd(η<sup>5</sup>-C<sub>5</sub>H<sub>5</sub>)(η<sup>3</sup>-1-PhC<sub>3</sub>H<sub>4</sub>)], which has been described by Baird and co-workers as a “stable precursor” for the preparation of Pd<sup>0</sup> complexes.<sup>[27]</sup> Upon addition of two equivalents of phosphine the allyl and cyclopentadienyl (Cp) fragments undergo reductive elimination to give the Pd<sup>0</sup>(PR<sub>3</sub>)<sub>2</sub> complexes (and organic byproducts). The reaction of **1** with [Pd(η<sup>5</sup>-C<sub>5</sub>H<sub>5</sub>)(η<sup>3</sup>-1-PhC<sub>3</sub>H<sub>4</sub>)] gave a single complex as judged by <sup>1</sup>H and <sup>31</sup>P NMR spectroscopy (Scheme 4). Two phosphorus doublet signals at δ = 31.2 and 13.2 ppm (<sup>2</sup>*J*<sub>PP</sub> = 20.5 Hz) suggest that the ligand is coordinated unsymmetrically to Pd. <sup>1</sup>H NMR spectroscopic analysis reveals two broad coupled olefin protons shifted upfield at δ = 5.28 and 5.95 ppm (confirmed by COSY), suggesting that an exchange process is occurring.



Scheme 4. Synthesis of  $[\text{Pd}^0_2(\mathbf{1})_2]$ .

Cooling the sample to 255 K sharpened the proton signals and a more complex spin–spin coupling network was revealed, namely a doublet of doublets (dd;  $\delta=5.3$  ppm) and doubled doublet of doublets (ddd;  $\delta=5.9$  ppm). Thus the olefin signal at  $\delta=5.9$  ppm is coupling to two phosphorus nuclei and that at  $\delta=5.3$  ppm to one phosphorus nuclei. Conclusive evidence confirming a Pd–olefin bonding interaction was provided by  $^{13}\text{C}$  NMR and HSQC spectra, which showed the olefin carbons associated with these upfield olefin protons had also shifted upfield to  $\delta=83$  and 69 ppm, respectively.

The UV/Vis spectrum supports the presence of a Pd–olefin bonding interaction. A metal-to-ligand charge transfer (MLCT) band at 454 nm,  $\epsilon=7088\text{ mol}^{-1}\text{ dm}^3\text{ cm}^{-1}$  ( $\text{CH}_2\text{Cl}_2$ ) is observed. This value sits between those recorded for  $[\text{Pd}(\eta^2\text{-dba})(\text{PPh}_3)_2]$  (396 nm, DMF, 405 nm MeOH)<sup>28</sup> and  $[\text{Pd}_2(\text{dba})_3]$  (530 nm, MeOH).<sup>[29]</sup>

$^{31}\text{P}$ – $^{31}\text{P}$  exchange spectroscopy (EXSY) experiments were used to obtain rate constants for the exchange process by varying the mixing time (d8) at different temperatures (Figure 5).<sup>[30]</sup> The exchange processes are affected by temperature to a greater extent than nOe processes, allowing the exchange to be frozen out. At 268 K no nOe cross-peaks

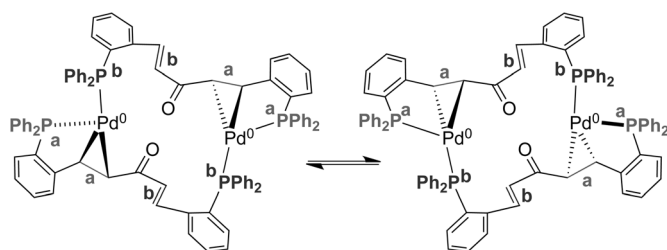


Figure 5. Dynamic exchange in  $[\text{Pd}^0_2(\mathbf{1})_2]$ .

were observed on irradiating at  $\delta=31.2$  ppm, allowing the exchange processes to be observed exclusively. An Arrhenius plot of  $1/T$  against  $\ln 2k$  gave a straight line with slope  $-E_a/R$ , allowing the activation energy to be estimated ( $68.2\text{ kJ mol}^{-1}$ ). Using the Eyring equation, the enthalpy and entropy of activation were calculated;  $\Delta H^\ddagger=(65.7\pm 3.4)\text{ kJ mol}^{-1}$  and  $\Delta S^\ddagger=(-19.5\pm 11.1)\text{ J mol}^{-1}\text{ K}^{-1}$ . The small value for  $\Delta S^\ddagger$  is in keeping with the exchange being intra-

molecular, with the barrier to exchange being explained by enthalpic differences. The free energy of activation ( $\Delta G^\ddagger$ ) at 298 K was determined to be  $(71.5\pm 4.7)\text{ kJ mol}^{-1}$ .

X-ray crystallographic analysis on a single crystal of  $[\text{Pd}^0_2(\mathbf{1})_2]$  allowed the structural connectivity to be determined<sup>[31]</sup> (Figure 6). The olefin C=C bond lengths indicate substantial back-bonding from  $\text{Pd}^0$  ( $\text{C}(7)\text{--}\text{C}(8)=1.435(11)\text{ \AA}$  and  $\text{C}(48)\text{--}\text{C}(49)=1.411(12)\text{ \AA}$ ; the C=C bond length in ligand  $\mathbf{1}=1.324(2)\text{ \AA}$ ). The bond lengths are similar to that

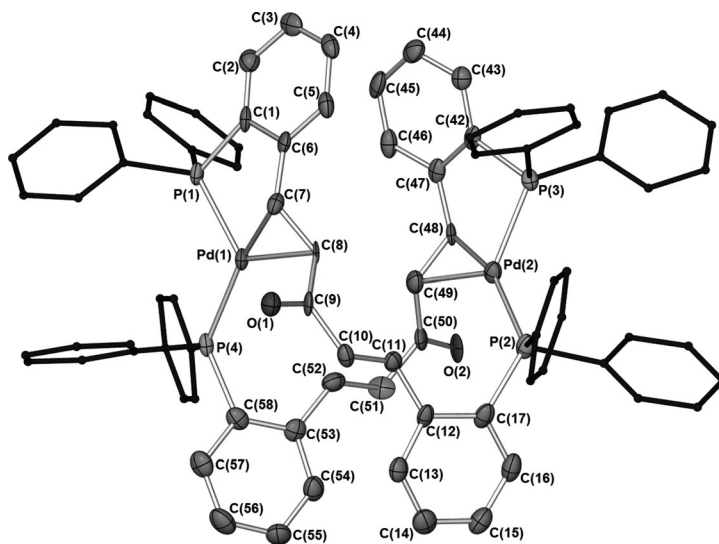


Figure 6. X-ray structure of  $[\text{Pd}^0_2(\mathbf{1})_2]$ .

found in the olefin–Pd interaction in  $[\text{Pd}(\eta^2\text{-dba})(\text{dppe})]$  ( $\text{dppe}=1,2\text{-bis}(\text{diphenylphosphino})\text{ethane}$ ),<sup>[32]</sup> which also shares similar Pd–P bond lengths.

The stoichiometric oxidative-addition reaction of iodobenzene and  $[\text{Pd}^0_2(\mathbf{1})_2]$  in  $[\text{D}_8]\text{THF}$  at 300 K was followed by NMR spectroscopy, taking approximately 1 h to reach completion (quantitative). The  $^{31}\text{P}$  NMR spectrum of the product showed one single  $^{31}\text{P}$  resonance ( $\delta=16.8$  ppm) indicating that the ligand was acting as a *trans*-spanning ligand. Four of the aromatic signals (from iodobenzene) in the  $^1\text{H}$  NMR spectrum appear significantly upfield, roughly between 5.9–6.4 ppm, which we interpret as being due to shielding from the phenyl rings of the phosphine, for example, sandwich-like  $\pi$ -stacking interactions,<sup>[33]</sup> leading us to propose *trans*- $[\text{Pd}^{\text{II}}\text{I}(\text{Ph})(\mathbf{1})]$  as the only isomer formed. Crystals suitable for X-ray diffraction were grown at 18 °C, which confirmed the *trans*-chelating nature of the dbaphos ligand  $\mathbf{1}$  (Figure 7). The P,P bite angle in this complex is  $172.37(3)^\circ$ , and the C(7)–H(7) bond points towards the  $\text{Pd}^{\text{II}}$  centre, the distance between the metal and hydrogen atoms is longer than in the *cis*- $[\text{PtCl}_2(\mathbf{1})]$ , complex, 2.90 versus 2.64 Å. The other ligand bond lengths (C=O, C=C and C–P) are within error of those in *cis*- $[\text{PtCl}_2(\mathbf{1})]$ . It is of particular note that the Morita–Bayliss–Hillman dimer diphosphine derived from the Lei ligand forms a similar *trans*- $\text{Pd}^{\text{II}}$  complex.<sup>[34]</sup>

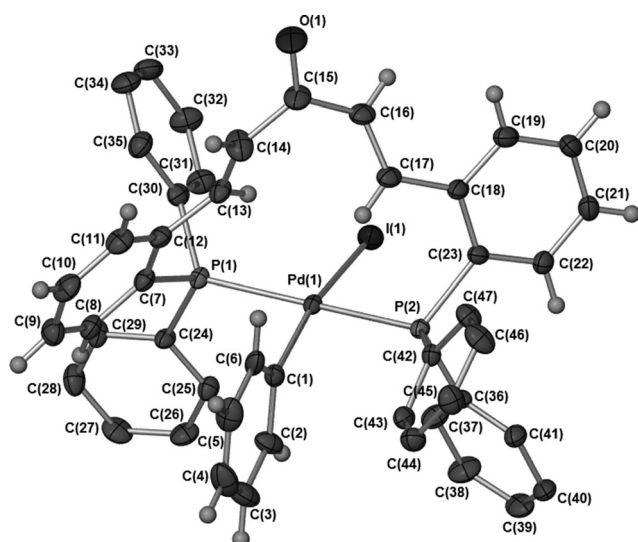
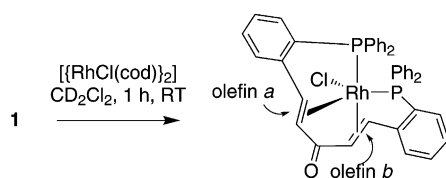


Figure 7. Single-crystal X-ray structure of *trans*-[Pd<sup>II</sup>(Ph)(1)]. Disordered solvent molecules (THF) and selected hydrogen atoms removed for clarity. Thermal ellipsoids shown at 50%. Selected bond lengths (Å) and bond angles (°): C(15)–O(1)=1.226(5), C(16)–C(17)=1.342(5), C(14)–C(13)=1.335(5), P(1)–C(7)=1.827(4), P(2)–C(23)=1.831(4), P(2)–Pd=2.3181(10), P(1)–Pd=2.3459(10), Pd–I=2.6810(5), Pd–C(1)=2.028(4); P(1)–Pd–P(2)=172.37(3).

Finally, we explored the reactivity of ligand **1** toward Rh<sup>I</sup>. The initial reaction of [RhCl(cod)]<sub>2</sub> (cod=1,5-cyclooctadiene) with **1** in CD<sub>2</sub>Cl<sub>2</sub> was monitored by <sup>1</sup>H and <sup>31</sup>P NMR spectroscopy (Scheme 5, showing the major product, 95% conversion).



Scheme 5. Synthesis of [RhCl(1)], a Rh<sup>I</sup> complex containing dbaphos (1).

Two products were formed in an approximate 95:5 ratio (in quantitative conversion). A similar outcome was noted in [D<sub>6</sub>]benzene (ca. 93:7). Leaving these reactions to run overnight led to the formation of other minor products, which we believe are due to interference of the cod ligand. After two weeks an orange precipitate was formed, which was filtered and shown to be a mixture of products in a ratio 93:7. Running a reaction with [Rh(η<sup>2</sup>-C<sub>2</sub>H<sub>4</sub>)<sub>2</sub>Cl]<sub>2</sub> in toluene gave the same products (ca. 93:7). So, irrespective of the Rh precursor the outcome is essentially the same.

The <sup>1</sup>H and <sup>31</sup>P NMR spectra are quite broad at 295 K due to exchange processes (Berry pseudorotation; Figure 8). Cooling the sample sharpened the proton signals and revealed the spin–spin multiplicities of the olefin protons. The two olefin protons at δ=3.6 and 2.6 ppm (olefin *a*) are

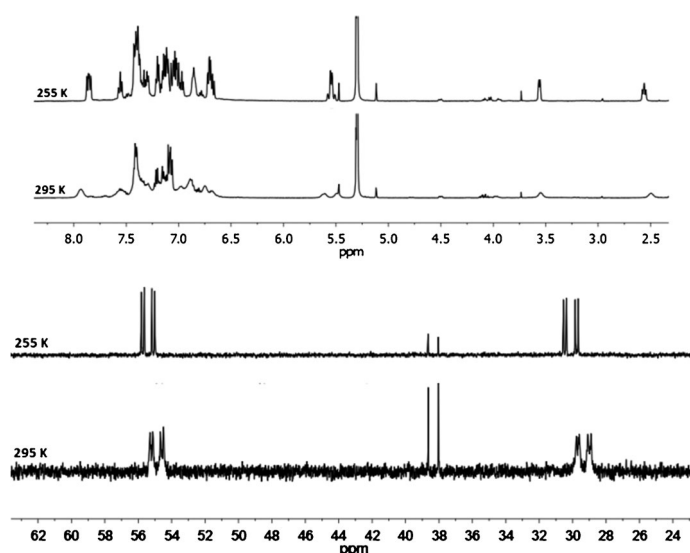


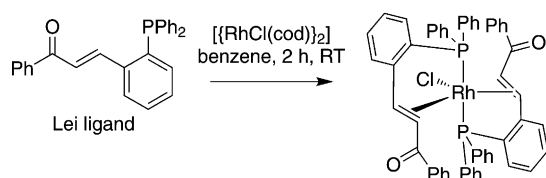
Figure 8. NMR spectra of [RhCl(1)] in CD<sub>2</sub>Cl<sub>2</sub>. Top: <sup>1</sup>H NMR spectra; bottom: variable-temperature <sup>31</sup>P NMR spectra.

COSY-correlated and their large upfield shifts from the free ligand olefin protons (Δδ=−4.7 and −4.2 ppm, respectively) are evidence for strong olefin binding to Rh<sup>I</sup>.

The two other olefin protons (olefin *b*) have shifted by Δδ=−2.7 and −1.2 ppm. The spin–spin coupling constants have decreased in both cases from 16 Hz to 13.5 Hz (olefin *b*) and roughly 7 Hz (olefin *a*)—a clear indication of Rh–olefin binding and a five-coordinate structure. The <sup>31</sup>P NMR spectrum exhibits two sharp doublet of doublet phosphorus signals (at 255 K) for the major product at δ=55.3 ppm (<sup>1</sup>J<sub>Rh,P<sub>a</sub></sub>=128 Hz, <sup>2</sup>J<sub>P<sub>a</sub>,P<sub>b</sub></sub>=36 Hz) and 30.0 ppm (<sup>1</sup>J<sub>Rh,P<sub>b</sub></sub>=144 Hz, <sup>2</sup>J<sub>P<sub>a</sub>,P<sub>b</sub></sub>=36 Hz) (Figure 8, bottom spectrum). The minor product exhibits a signal at δ=38.3 ppm (<sup>1</sup>J<sub>Rh,P</sub>=124 Hz), the structure of which cannot be determined from the available data. Previous work with phosphino–olefin ligands and five-coordinate trigonal bipyramidal Rh<sup>I</sup> complexes has demonstrated that olefins preferentially bind in the equatorial plane.<sup>[35]</sup> From the <sup>31</sup>P<sub>a</sub>,<sup>31</sup>P<sub>b</sub> spin–spin coupling constant of 36 Hz it is clear that the phosphines are not *trans* to one another, as much larger coupling constants are observed (ca. 300 Hz).<sup>[36]</sup> As olefins prefer the equatorial plane it would seem logical to place one phosphine group and chloride ion in axial positions, with the remaining phosphine in the equatorial plane. However, the large difference in the chemical shifts of the two coordinated olefins needs to be factored in. Crucially, with the data in hand, it is not possible to ascertain the two positions of the olefins (note: attempts to crystallise [RhCl(1)] failed). There is also the possibility of a dinuclear structure, although molecular models, and comparison with the X-ray structure of [Pd<sup>0</sup><sub>2</sub>(1)<sub>2</sub>], indicate that it is unlikely.<sup>[37]</sup>

Preliminary diffusion ordered spectroscopy (DOSY) measurements (in  $\text{CD}_2\text{Cl}_2$ ), comparing the major species of  $[\text{Rh}^{\text{I}}\text{Cl}(\mathbf{1})]$  and  $[\text{Rh}^{\text{I}}\text{Cl}(\text{Lei})_2]$  have proven inconclusive.<sup>[38]</sup>

Further structural data could be obtained through the synthesis and characterisation of the  $\text{Rh}^{\text{I}}$  complex containing the Lei ligand. Reaction of the Lei ligand (hereafter referred to as “Lei”) with  $[\text{Rh}(\text{cod})\text{Cl}]_2$  (in a 2:1 molar ratio) in  $[\text{D}_6]$ benzene at ambient temperature gave a new complex,  $[\text{Rh}^{\text{I}}\text{Cl}(\text{Lei})_2]$ , in 71 % yield (Scheme 6).  $^1\text{H}$  and  $^{31}\text{P}$  NMR



Scheme 6. Synthesis of  $[\text{Rh}^{\text{I}}\text{Cl}(\text{Lei})_2]$ , a  $\text{Rh}^{\text{I}}$  complex containing two Lei ligands.

spectra ( $\text{CDCl}_3$ ) showed that two ligands were coordinated to  $\text{Rh}^{\text{I}}$  through both the olefin and phosphine groups (Figure 9). X-ray crystallography on a single crystal of

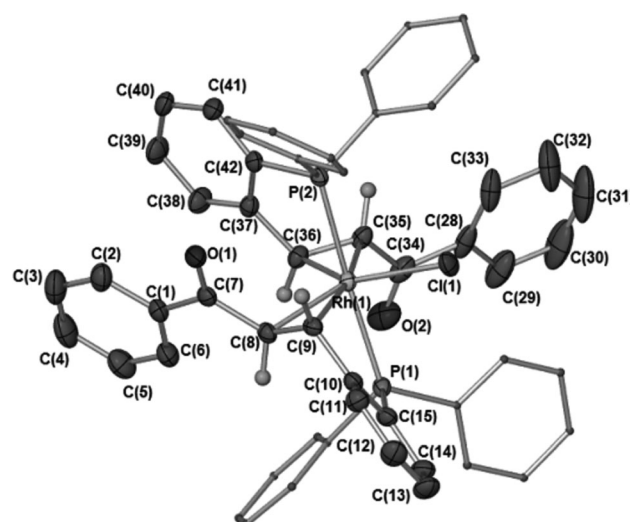


Figure 10. X-ray structure of  $[\text{Rh}^{\text{I}}\text{Cl}(\text{Lei})_2]$ .

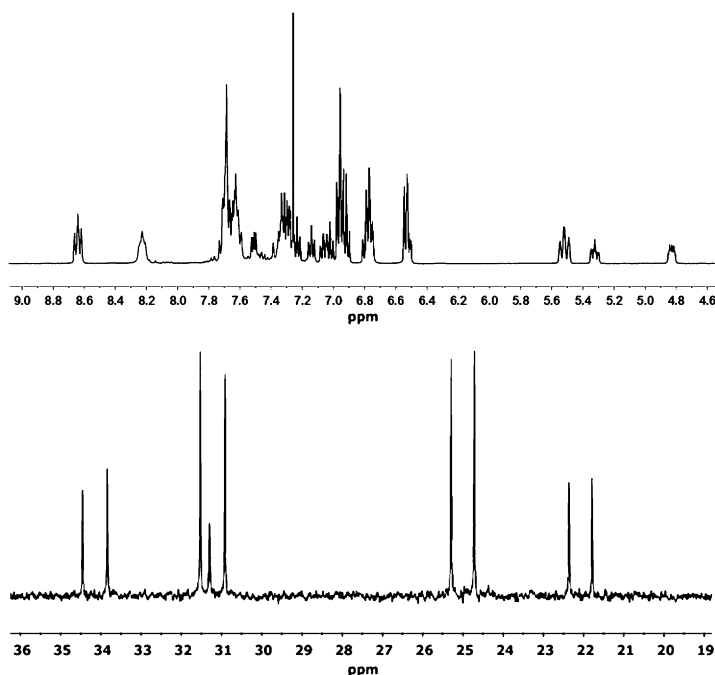


Figure 9. NMR spectra of  $[\text{Rh}^{\text{I}}\text{Cl}(\text{Lei})_2]$  in  $\text{CDCl}_3$  (298 K): Top:  $^1\text{H}$  NMR spectrum; bottom:  $^{31}\text{P}$  NMR spectrum (note: the peak at ca.  $\delta = 31.4$  ppm is trace phosphine oxide of the free ligand).

$[\text{Rh}^{\text{I}}\text{Cl}(\text{Lei})_2]$  revealed that the two phosphine groups are positioned *trans* in axial positions, whereas the two olefins and chloride ligands are found in the equatorial positions (Figure 10). The  $^1\text{H}$  NMR spectrum further showed that both olefins (non-identical in solution) are found at approxi-

mately  $\delta = 4.8\text{--}5.6$  ppm (one overlapping signal and two partially-resolved signals).  $^{31}\text{P}$  NMR spectroscopic analysis of  $[\text{Rh}^{\text{I}}\text{Cl}(\text{Lei})_2]$  shows two doublet of doublets signals (note: ABX system). The spin-spin coupling-constant values for the two doublets differ slightly, highlighting a small difference in the chemical environments of the two phosphorus atoms. The chemical shift of  $\text{P}_a$  is  $\delta = 24.3$ , with spin-spin coupling constants of  $J_{\text{P}_a\text{P}_b} = 474$  Hz and  $J_{\text{RhP}_a} = 93$  Hz. The chemical shift of  $\text{P}_b$  is  $\delta = 31.8$  ppm, with spin-spin coupling constant values of  $J_{\text{P}_b\text{P}_a} = 474$  Hz and  $J_{\text{RhP}_b} = 100$  Hz. The  $J_{\text{RhP}}$  coupling values correspond well with those reported for axially-disposed phosphines in  $[\text{RhCl}(\text{PMe}_3)_3]$  complexes containing a  $\pi$ -bound diyne (ca. 97 Hz).<sup>[39]</sup> The origin of the phosphorus inequivalence in solution is not clear. Also, to the best of our knowledge, the  $J_{\text{P}_b\text{P}_a}$  coupling is one of the highest ever recorded for a  $\text{Rh}^{\text{I}}$  complex.

Thus, from the  $^{31}\text{P}$  NMR spectroscopic analysis of  $[\text{RhCl}(\text{Lei})_2]$  we predict that  $\text{P}_a$  in  $[\text{Rh}^{\text{I}}\text{Cl}(\mathbf{1})]$  is located in the equatorial position (higher chemical shift) and  $\text{P}_b$  in the axial position (similar to the P atoms in  $[\text{Rh}^{\text{I}}\text{Cl}(\text{Lei})_2]$ ). The structural connectivity proposed in Scheme 5 for  $[\text{RhCl}(\mathbf{1})]$  is most likely from the evidence available. DFT calculations (B3LYP) provide further support the proposed structure. Three conformations about the 1,4-dien-3-one moiety are possible, with *s-trans,s-trans* and pseudo-*s-cis,s-trans* being most feasible (Figure 11). The former conformer was found to be 4 kcal mol<sup>−1</sup> lower in relative free energy than the pseudo-*s-cis,s-trans*. Indeed a *s-trans,s-trans* ligated dba was found viable in  $[\text{Rh}(\eta^5\text{-C}_5\text{Me}_5)(\eta^2,\eta^2\text{-dba-H})]$ .<sup>[1]</sup> The coordinated olefins show a significant increase in bond length for the equatorially bound olefin (equatorial olefin C=C bond length = 1.466 Å; axial olefin C=C bond length = 1.402 Å). This difference adequately accounts for the substantially shielded olefin *a* protons observed in NMR spectra of  $[\text{RhCl}(\mathbf{1})]$ . The differences observed between the  $[\text{RhCl}(\mathbf{1})]$  and  $[\text{RhCl}(\text{Lei})_2]$  complexes can be explained by the former



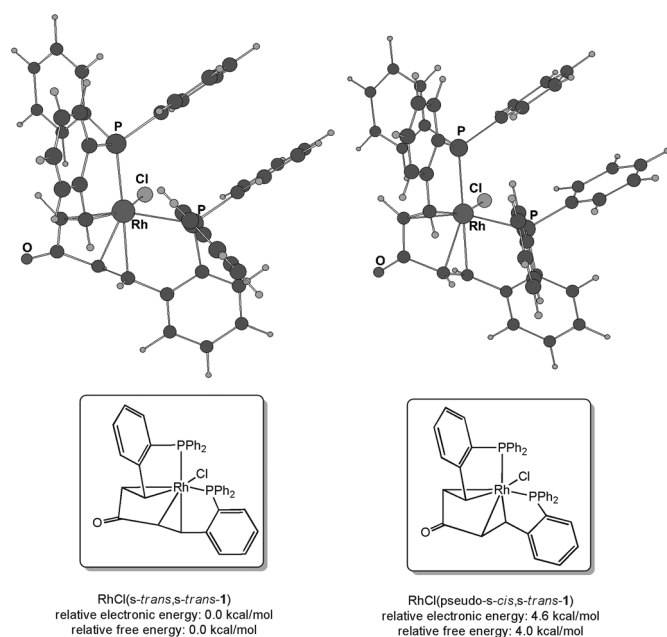


Figure 11. DFT-calculated structures of  $[\text{RhCl}(\textit{s-trans,s-trans-1})_2]$  and  $[\text{RhCl}(\textit{pseudo-s-cis,s-trans-1})_2]$ .

having *cis*-phosphines, whereas the latter has *trans*-phosphines, in addition to the olefins being *s-trans* and not *s-cis*.

## Conclusion

In conclusion, dbaphos **1** is a flexible multidentate ligand which is capable of forming both *cis*- and *trans*-metal complexes.<sup>[15,40]</sup> It also serves as a bridging ligand, in which the olefin interactions with  $\text{Pd}^0$  have been noted. In the case of  $\text{Rh}^I$ , ligand **1** is able to coordinate through two phosphines and two olefins, a quite remarkable finding, which highlights the flexibility and diversity of coordination modes that are accessible using the dbaphos ligand. Moreover, the “extreme-back-bonding” for olefin *a* in  $[\text{RhCl}(\textbf{1})]$  indicates that the Rh centre is closer to a +III oxidation state, which stands in contrast with the  $[\text{RhCl}(\text{Lei})_2]$  complex (in which less back-bonding was found to occur). We believe the coordination chemistry detailed herein could be exploited in various transition-metal-catalysed processes.

## Experimental Section

**General details:** See Supporting Information, which includes details of the compound synthesis, characterisation (including known compounds) and representative NMR spectra. Details for all novel compounds are given below. See the Supporting Information for the NMR structural assignments. CCDC-905779 (**1**), 905778 (*cis*- $[\text{PtCl}_2(\textbf{1})]$ ), 914497 ( $[\text{Pd}_2(\textbf{1})_2]$ ), 905781 (*trans*- $[\text{PdI}(\text{Ph})(\textbf{1})]$ ) and 905780 ( $[\text{RhCl}(\text{Lei})_2]$ ) contain the supplementary crystallographic data for this paper. These data can be obtained free of charge from The Cambridge Crystallographic Data Centre via [www.ccdc.cam.ac.uk/data\\_request/cif](http://www.ccdc.cam.ac.uk/data_request/cif).

**(1*E,4E*)-1,4-Di[2-(1,1-diphenylphosphino)phenyl]-1,4-pentadien-3-one, dbaphos, (**1**):** Dry and degassed THF (17 mL) was added by cannula to an  $\text{N}_2$ -flushed Schlenk containing *o*-diphenylphosphinobenzaldehyde (2.09 g, 2 equiv, 7.2 mmol). 1,3-Bis(diethoxyphosphonato)acetone (see Supporting Information for preparation of this compound) (1.55 g, 1.2 equiv, 4.7 mmol) was added dropwise and a yellow solution formed on stirring. A solution of NaOH (576 mg, 4 equiv, 14.4 mmol) in degassed water (2.2 mL) was added dropwise. The resulting mixture was stirred vigorously for 2–3 h at 80 °C (the reaction could be followed by  $^{31}\text{P}$  NMR spectroscopy and additional 1,3-bis(diethoxyphosphonato)acetone added if needed). Saturated  $\text{N}_2$ -purged  $\text{NH}_4\text{Cl}$  (5 mL) was added to the mixture, followed by degassed  $\text{H}_2\text{O}$  (5 mL) and the aqueous layer extracted with dry and degassed  $\text{CH}_2\text{Cl}_2$  ( $3 \times 10$  mL until the  $\text{CH}_2\text{Cl}_2$  layer remained colourless) and the organic layer transferred by cannula to a Schlenk containing dry  $\text{Na}_2\text{SO}_4$ . After filtration under  $\text{N}_2$ , the solvent was removed in vacuo, to give a yellow oily solid that turned to green oil overnight. The green oil was redissolved in dry and degassed  $\text{Et}_2\text{O}$ , washed with degassed  $\text{H}_2\text{O}$ , transferred to a Schlenk containing dry  $\text{Na}_2\text{SO}_4$ , filtered by cannula under  $\text{N}_2$  and the solvent removed to give the product as a solid (1.81 g, 84%, >96% pure by  $^{31}\text{P}$  NMR; note: if benzaldehyde remains, column chromatography on silica gel eluting with  $\text{Et}_2\text{O}$ /hexane (20:80 v/v) under  $\text{N}_2$  can be used to purify the product. The benzaldehyde is the first yellow band and the second bright yellow band is the product). Mp. 67 °C (decomp);  $^1\text{H}$  NMR (400 MHz,  $\text{CD}_2\text{Cl}_2$ ):  $\delta$  = 8.30 (dd,  $J$  = 16.0, 5.0 Hz, 2H;  $\text{H}_\text{c}$ ), 7.69 (dddd,  $J$  = 8.0, 4.5, 1.5, 0.5 Hz, 2H;  $\text{H}_\text{h}$ ), 7.44–7.39 (m, 2H;  $\text{H}_\text{g}$ ), 7.37–7.21 (m, 22H;  $\text{H}_\text{i}$  and Ar), 6.96 (ddd,  $J$  = 7.5, 4.5, 1.5 Hz, 2H;  $\text{H}_\text{e}$ ), 6.78 ppm (dd,  $J$  = 16.0, 1.5 Hz, 2H;  $\text{H}_\text{b}$ );  $^{13}\text{C}$  NMR (100 MHz,  $\text{CD}_2\text{Cl}_2$ ):  $\delta$  = 188.7 ( $\text{C}_\text{a}$ ), 141.4 (d,  $J$  = 26 Hz;  $\text{C}_\text{c}$ ), 139.7 (d,  $J$  = 22 Hz; *ipso*-C), 138.8 (d,  $J$  = 16 Hz; *ipso*-C), 136.3 (d,  $J$  = 10 Hz;  $\text{C}_\text{d}$ ), 134.3 (d,  $J$  = 20 Hz; Ar), 134.0 ( $\text{C}_\text{e}$ ), 130.3 (d,  $J$  = 1 Hz;  $\text{C}_\text{g}$ ), 129.5 ( $\text{C}_\text{f}$ ), 129.3 (*p*-C), 129.0 (d,  $J$  = 7 Hz; Ar), 127.2 (d,  $J$  = 3 Hz;  $\text{C}_\text{b}$ ), 127.0 ppm (d,  $J$  = 4 Hz;  $\text{C}_\text{h}$ );  $^{31}\text{P}$  NMR (162 MHz,  $\text{CD}_2\text{Cl}_2$ ):  $\delta$  = –14.09 ppm (s); IR (ATR):  $\tilde{\nu}$  = 3051 (w), 2962 (w), 1654 (w), 1614 (w), 1596 (w), 1457 (w), 1434 (w), 1325 (br, w), 1260 (w), 1182 (w), 1093 (m), 1026 (w), 975 (w), 799 (br, w), 741 (s), 694  $\text{cm}^{-1}$  (s); HRMS (ESI):  $m/z$  calcd for  $\text{C}_{41}\text{H}_{33}\text{O}_2$ : 603.2001 [ $M < M + > \text{H}$ ] $^+$ ; found: 603.1993; elemental analysis calcd (%) for  $\text{C}_{41}\text{H}_{32}\text{O}_2$  (602): C 81.71, H 5.36; found: C 80.82, H 5.40 (the compound is being oxidised during the elemental analysis—the calculated results for 20% oxidation match those observed; elemental analysis calcd (%) for 20% phosphine oxide: C 80.86, H 5.30).

***cis*- $[\text{PtCl}_2(\textbf{1})]$ :**  $[\text{PtCl}_2(\text{cod})]$  (125 mg, 1 equiv, 0.33 mmol) was added to a solution of dbaphos (**1**) (200 mg, 1 equiv, 0.33 mmol) in dry and degassed  $\text{CH}_2\text{Cl}_2$  (5 mL). The solution was stirred for 1 h under  $\text{N}_2$  at room temperature. A pale yellow precipitate formed.  $\text{Et}_2\text{O}$  (2 mL) was added and the mixture filtered through a funnel with a sintered glass frit and washed with  $\text{Et}_2\text{O}$  (15 mL) to afford the product as a pale yellow powder (224 mg, 78%). Mp. 140 °C (decomp);  $^1\text{H}$  NMR (400 MHz,  $\text{CD}_2\text{Cl}_2$ ):  $\delta$  = 9.82 (d,  $J$  = 16.5 Hz, 2H;  $\text{H}_\text{c}$ ), 7.88–7.81 (m, 4H; *o*-Ph), 7.78 (dd,  $J$  = 8.0, 4.0 Hz, 2H; Ar), 7.61–7.55 (m, 2H; *p*-Ph), 7.52–7.43 (m, 8H; *m*-Ph and Ar), 7.38–7.23 (m, 2H; Ar), 7.05–6.98 (m, 2H; *p*-Ph), 6.91–6.82 (m, 4H; *o*-Ph), 6.74–6.65 ppm (m, 6H;  $\text{H}_\text{b}$  and *m*-Ph);  $^{31}\text{P}$  NMR (162 MHz,  $\text{CD}_2\text{Cl}_2$ ):  $\delta$  = 4.72 ppm (s,  $^1J_{\text{Pt,P}} = 3562$  Hz); IR (KBr):  $\tilde{\nu}$  = 3680–3300 (w, br,  $\text{H}_2\text{O}$ ), 3055 (m), 3020 (w), 1635 (s), 1616 (s), 1586 (w), 1481 (m), 1461 (m), 1434 (s), 1313 (w), 1293 (m), 1271 (m), 1199 (w), 1188 (w), 1121 (w), 1096 (s), 998 (w), 968 (m), 904 (w), 886 (w), 876 (w), 846 (w), 760 (s), 745 (s), 693 (s), 570 (m), 548 (s), 517 (s), 475  $\text{cm}^{-1}$  (w); HRMS (ESI):  $m/z$  calcd for  $\text{C}_{41}\text{H}_{32}\text{Cl}_2\text{OPt}$ : 868.1026 [ $M < M + > \text{H}$ ] $^+$ ; found: 868.1046;  $m/z$  calcd for  $\text{C}_{41}\text{H}_{31}\text{OPt}$ : 796.1492 [ $M - \text{HCl}$ ] $^+$ ; found 796.1467; elemental analysis calcd (%) for  $\text{C}_{41}\text{H}_{32}\text{O}_2\text{PtCl}_2 \cdot \text{H}_2\text{O}$  (868): C 55.54, H 3.87; found: C 55.70, H 3.62 (water is observed in the IR spectrum); solid-state CPMAS-NMR:  $^{31}\text{P}$  NMR (162 MHz):  $\delta$  = 4.4 ( $^1J_{\text{Pt,P}} = 3590$  Hz), 1.9 ppm ( $^1J_{\text{Pt,P}} = 3590$  Hz);  $^{13}\text{C}$  NMR (101 MHz):  $\delta$  = 192.2, 145.2, 141.5, 139.3, 138.3, 135.8, 134.0, 132.9, 129.6, 125.6 ppm; In  $[\text{D}_6]\text{DMSO}$   $^{31}\text{P}$  NMR (162 MHz,  $[\text{D}_6]\text{DMSO}$ ):  $\delta$  = 15.33 ( $^1J_{\text{Pt,P}} = 2565$  Hz, *trans*- $[\text{PtCl}_2(\textbf{1})]$ ), 4.68 ppm ( $^1J_{\text{Pt,P}} = 3554$  Hz, *cis*- $[\text{PtCl}_2(\textbf{1})]$ ); after heating at 60 °C for 4 h only the *trans*- $[\text{PtCl}_2(\textbf{1})]$  was observed:  $^1\text{H}$  NMR (400 MHz,  $[\text{D}_6]\text{DMSO}$ ):  $\delta$  = 8.81 (d,  $J$  = 16.5 Hz, 2H), 8.20 (d,  $J$  = 8.0 Hz, 2H), 7.98–7.27 (m, 22H), 7.14–7.04 (m, 2H), 6.97 (d,  $J$  = 16.5 Hz, 2H), 6.87–6.78 ppm (m, 2H);



$^{31}\text{P}$  NMR (162 MHz,  $[\text{D}_6]\text{DMSO}$ )  $\delta$  = 15.33 ppm ( $^1J_{\text{Pt,P}}$  = 2565 Hz); a minor product was also observed in the  $^{31}\text{P}$  NMR spectrum  $\delta$  = 43.04 (d,  $^2J_{\text{PP}}$  = 12 Hz), 20.32 ppm (d,  $^2J_{\text{PP}}$  = 12 Hz), containing no Pt satellites.

**trans-[PtCl<sub>2</sub>(1)]**: A solution of dbaphos **1** (20 mg, 1 equiv, 0.033 mmol) in dry and degassed  $\text{CD}_2\text{Cl}_2$  (0.8 mL) was added to *trans*-[PtCl<sub>2</sub>(MeCN)<sub>2</sub>] (12 mg, 1 equiv, 0.033 mmol) in a glove-box. The reaction was monitored by  $^1\text{H}$  and  $^{31}\text{P}$  NMR spectroscopy. A pale yellow precipitate formed. After 3 h the precipitate was collected by filtration, washed with  $\text{Et}_2\text{O}$  (5 mL) and dried in vacuo to give a pale yellow solid (14 mg, 50%). M.p. > 230 °C (decomp);  $^1\text{H}$  NMR (500 MHz,  $\text{CD}_2\text{Cl}_2$ ):  $\delta$  = 8.90 (d,  $J$  = 16.5 Hz, 2H;  $\text{H}_\text{c}$ ), 7.98 (d,  $J$  = 8.0 Hz, 2H; Ar), 7.71–7.62 (m, 8H; Ph), 7.51–7.46 (m, 6H; *p*-Ph and Ar), 7.43–7.36 (m, 8H; Ph), 7.30–7.23 (m, 2H; Ar), 6.93 (dtd,  $J$  = 7.0, 5.5, 1.0 Hz, 2H; Ar), 6.78 ppm (d,  $J$  = 16.5 Hz, 2H;  $\text{H}_\text{b}$ );  $^{31}\text{P}$  NMR (202 MHz,  $\text{CD}_2\text{Cl}_2$ ):  $\delta$  = 14.89 ppm ( $^1J_{\text{Pt,P}}$  = 2577 Hz); IR (KBr):  $\tilde{\nu}$  = 3680–350 (w, br,  $\text{H}_2\text{O}$ ), 3053 (m), 1634 (s), 1560 (w), 1478 (w), 1462 (m), 1432 (s), 1301 (m), 1274 (w), 1202 (m), 1122 (w), 1095 (m), 970 (m), 770 (w), 750 (m), 740 (w), 705 (m), 692 (s), 570 (w), 514 (s), 485  $\text{cm}^{-1}$  (w); MS (LIFDI):  $m/z$  (%): 868.05 (28) [ $\text{M}]^+$ , 832.02 (12) [ $\text{M}-\text{Cl}]^+$ , 795.11 (100) [ $\text{M}-\text{HCl}_2$ ] $^+$ ; HRMS (ESI):  $m/z$  calcd for  $\text{C}_{41}\text{H}_{32}\text{OPt}$ : 796.1496 [ $\text{M}-\text{HCl}_2$ ] $^+$ ; found: 796.1470.

**[Pd<sup>0</sup><sub>2</sub>(1)<sub>2</sub>]**: Dry and degassed  $\text{CH}_2\text{Cl}_2$  (3.5 mL) was added to a Schlenk tube containing dbaphos, **1** (100 mg, 1 equiv, 0.17 mmol) and  $[\text{Pd}(\eta^5\text{-C}_5\text{H}_5)\{\eta^3\text{-1-Ph}(\text{C}_5\text{H}_4)\}]$  (47 mg, 1 equiv, 0.17 mmol), and the resulting mixture was stirred at room temperature for 2 h. The solvent was then removed in vacuo to give a red solid. Dry and degassed  $\text{Et}_2\text{O}$  (8 mL) was added and the mixture stirred to dissolve any remaining organics. Filtration by cannula, followed by drying the solid in vacuo gave the product as a red/purple solid (79 mg, 66%). M.p. 188 °C (decomp);  $^1\text{H}$  NMR (500 MHz,  $\text{CD}_2\text{Cl}_2$ , 295 K):  $\delta$  = 8.92 (dd,  $J$  = 16.5, 4.5 Hz, 2H;  $\text{H}_\text{c}$ ), 7.47–6.67 (m, 56H; Ar), 5.95 (m with underlying d,  $J$  = 16.5 Hz, 4H;  $\text{H}_\text{j}$  and  $\text{H}_\text{d}$ ), 5.28 ppm (dd,  $J$  = 11.5, 8.0 Hz, 2H;  $\text{H}_\text{b}$ );  $^{13}\text{C}$  NMR (126 MHz,  $\text{CD}_2\text{Cl}_2$ ):  $\delta$  = 185.7 ( $\text{C}_\text{c}$ ), 134.6 (d,  $J$  = 17 Hz), 133.9 (d,  $J$  = 16 Hz), 133.1, 132.6 (d,  $J$  = 13 Hz;  $\text{C}_\text{d}$ ), 131.2 ( $\text{C}_\text{j}$ ), 130.6, 129.9, 129.6, 129.3, 128.9 (d,  $J$  = 9 Hz), 128.7–128.5 (m), 128.2 (d,  $J$  = 10 Hz), 127.7 (d,  $J$  = 5 Hz), 82.9 (d,  $J$  = 21 Hz;  $\text{C}_\text{g}$ ), 69.5–69.2 ppm (m;  $\text{C}_\text{h}$ );  $^{31}\text{P}$  NMR (202 MHz,  $\text{CD}_2\text{Cl}_2$ ):  $\delta$  = 31.15 (d,  $J$  = 20.5 Hz), 13.19 ppm (d,  $J$  = 20.5 Hz); IR (KBr):  $\tilde{\nu}$  = 3050 (w), 1653 (m), 1588 (m), 1478 (m), 1457 (m), 1433 (s), 1298 (m), 1209 (w), 1180 (w), 1118 (w), 1093 (m), 1026 (w), 998 (w), 968 (w), 830 (w), 742 (m), 693 (s), 574 (w), 505  $\text{cm}^{-1}$  (m); UV/Vis ( $\text{CH}_2\text{Cl}_2$ ):  $\lambda_{\text{max}}$  ( $\epsilon$ ) = 454 (7088), 284 nm (18951  $\text{mol}^{-1}\text{m}^2\text{cm}^{-1}$ ); HRMS (LIFDI):  $m/z$  (monomer) calcd for  $\text{C}_{41}\text{H}_{32}\text{OP}_2\text{Pd}$ : 708.0963 [ $\text{M}]^+$ ; found: 708.0887; elemental analysis calcd (%) for  $\text{C}_{41}\text{H}_{32}\text{OP}_2\text{Pd}$  (708): C 69.45 H 4.55; found: C 69.32 H 4.55. Crystals of  $[\text{Pd}^0_2(\text{1})_2]$  were obtained from  $\text{CD}_2\text{Cl}_2$  layered with  $\text{Et}_2\text{O}$  ( $\text{CD}_2\text{Cl}_2/\text{Et}_2\text{O}$ , 1:1, v/v).

**trans-[PdI(Ph)(1)]**: Iodobenzene (1.8  $\mu\text{L}$ , measured as 1 equiv) was added under a flow of Ar to a solution of  $[\text{Pd}^0_2(\text{1})_2]$  (11.6 mg, 1 equiv, 0.015 mmol) in  $[\text{D}_8]\text{THF}$  (0.8 mL) in a Young's tap NMR tube. The reaction was monitored by  $^1\text{H}$  and  $^{31}\text{P}$  NMR spectroscopy. After 1 h the oxidative addition was complete (100% conversion by  $^{31}\text{P}$  NMR spectroscopy).  $^1\text{H}$  NMR (500 MHz,  $[\text{D}_8]\text{THF}$ ):  $\delta$  = 8.88 (d,  $J$  = 16.5 Hz, 2H;  $\text{H}_\text{c}$ ), 8.02–7.91 (m, 6H; Ar), 7.41–7.30 (m, 8H; Ar), 7.24 (apparent t,  $J$  = 7.5 Hz, 2H; Ar), 7.17 (d,  $J$  = 7.5 Hz, 1H;  $\text{H}_\text{d}$ ), 7.09–7.04 (m, 6H; Ar), 7.01–6.95 (m, 4H; Ar), 6.93–6.84 (m, underlying d,  $J$  = 16.5 Hz, 4H;  $\text{H}_\text{b}$  and Ar), 6.42 (apparent t,  $J$  = 7.5 Hz, 1H;  $\text{H}_\text{n}$ ), 6.36 (apparent t,  $J$  = 7.5 Hz, 1H;  $\text{H}_\text{m}$ ), 6.15 (apparent d,  $J$  = 7.5 Hz, 1H;  $\text{H}_\text{e}$ ), 5.95 ppm (apparent t,  $J$  = 7.5 Hz, 1H;  $\text{H}_\text{j}$ );  $^{31}\text{P}$  NMR (202 MHz,  $[\text{D}_8]\text{THF}$ ):  $\delta$  = 16.83 ppm (s); MS (LIFDI):  $m/z$  (%): 911.06 (8) [ $\text{M}]^+$  {isotope pattern 908.99 (24), 910.12 (47), 911.10 (86), 912.01 (40), 913.08 (100), 914.07 (25), 915.08 (21)}, 784.14 (100) [ $\text{M}-\text{I}]^+$  {isotope pattern: 782.14 (17), 783.15 (58), 784.14 (100), 786.13 (67), 788.14 (25), 789.45 (8)}, 706.09 (31), 679.26 (44); HRMS (LIFDI):  $m/z$  calcd for  $\text{C}_{47}\text{H}_{36}\text{OP}_2\text{Pd}$ : 784.1276 [ $\text{M}-\text{I}]^+$ ; found: 784.1377. Crystals of *trans*-[PdI(Ph)(1)], suitable for X-ray diffraction, were grown by cooling the reaction mixture to –18 °C ( $[\text{D}_8]\text{THF}$ ).

**[Rh<sup>1</sup>Cl(1)]**:  $[\text{Rh}_2(\mu\text{-Cl})_2(\text{C}_2\text{H}_4)_4]$  (32 mg, 0.5 equiv, 0.083 mmol) was placed in a Schlenk flask, evacuated and refilled with  $\text{N}_2$  three times, then dbaphos **1** (100 mg, 1 equiv, 0.166 mmol) was added (under a flow of  $\text{N}_2$ ). Dry and degassed toluene (5 mL) was added and the reaction mixture stirred. The reaction mixture goes from red to brown. After leav-

ing overnight a brown precipitate was collected by cannula filtration, (37 mg, 30%). M.p. 222–240 °C (decomp);  $^1\text{H}$  NMR (500 MHz,  $\text{CD}_2\text{Cl}_2$ , 255 K): major product (**A**)<sup>[40]</sup>  $\delta$  = 7.86 (dd,  $J$  = 11.0, 7.5 Hz, 2H; Ar), 7.56 (t,  $J$  = 8.0 Hz, 2H; Ar), 7.45–7.28 (m, 10H; Ar), 7.24–6.94 (m, 13H; Ar), 6.86 (t,  $J$  = 6.5 Hz, 2H; Ar), 6.75–6.65 (m, 3H; Ar), 5.57 (dd,  $J$  = 13.5, 2.5 Hz, 1H;  $\text{H}_\text{j}$ ), 5.52 (d,  $J$  = 13.5 Hz, 1H;  $\text{H}_\text{k}$ ), 3.56 (d,  $J$  = 6.5 Hz, 1H;  $\text{H}_\text{g}$ ), 2.56 ppm (dd,  $J$  = 8.5, 7.5 Hz, 1H;  $\text{H}_\text{b}$ ); minor product (**B**) visible peaks  $\delta$  = 7.51–7.45 (m, 1H), 6.83–6.75 (m, 1H), 4.51 (dd,  $J$  = 10.5, 3.0 Hz, 0.2H), 3.94 ppm (dd,  $J$  = 10.0, 5.5 Hz, 0.2 Hz);  $^{31}\text{P}$  NMR (202 MHz,  $\text{CD}_2\text{Cl}_2$ , 255 K):  $\delta$  = 55.32 (dd,  $^1J_{\text{Rh,P}}$  = 128.0,  $^2J_{\text{PP}}$  = 35.5 Hz, 0.97P), 38.27 (d,  $^1J_{\text{Rh,P}}$  = 124.0 Hz, 0.03P), 30.04 ppm (dd,  $^1J_{\text{Rh,P}}$  = 143.5,  $^2J_{\text{PP}}$  = 35.5 Hz, 0.97P); IR (KBr):  $\tilde{\nu}$  = 3051 (w), 1628 (w, br), 1554 (m), 1482 (m), 1454 (m), 1434 (s), 1419 (s), 1354 (w), 1291 (w), 1273 (w), 1246 (w), 1209 (m), 1187 (w), 1156 (w), 1120 (w), 1093 (m), 1068 (w), 1028 (w), 999 (w), 980 (w), 877 (w), 868 (w), 829 (w), 753 (m), 740 (m), 705 (m), 694 (s), 657 (w), 626 (w), 592 (w), 534 (m), 517 (m), 505 (s), 464  $\text{cm}^{-1}$  (w); HRMS (ESI):  $m/z$  calcd for  $\text{C}_{41}\text{H}_{32}\text{OP}_2\text{Rh}$ : 705.0978 [ $\text{M}-\text{Cl}]^+$ ; found 705.0948.

**[Rh<sup>1</sup>Cl(Lei)<sub>2</sub>]**: A solution of  $[\{\text{RhCl}(\text{cod})\}_2]$  (0.037 g,  $7.51 \times 10^{-5}$  mol) and “Lei” ligand (0.086 g, 0.22 mmol, ca. 1.5 equiv to Rh) in benzene (10 mL) was stirred for 2 h at ambient temperature. The solvent was removed and concentrated in vacuo to approximately 5 mL, which led to the precipitation of a light yellow microcrystalline solid (0.098 g, 71%). Mp 221–223 °C;  $^1\text{H}$  NMR (400 MHz,  $\text{CDCl}_3$ ):  $\delta$  = 8.64 (m, 2H), 8.23 (m, 2H), 7.58–7.74 (br m, 11H), 7.51 (dd,  $J$  = 7.5, 4.0 Hz, 1H), 7.20–7.38 (br m, 7H), 7.14 (t,  $J$  = 7.5 Hz, 1H), 7.00–7.09 (br m, 2H), 6.88–6.99 (br m, 5H), 6.78 (m, 4H), 6.53 (m, 3H), 5.52 (m, 2H), 5.32 (ddd,  $J$  = 10.5, 7.5, 2.5 Hz, 1H), 4.83 ppm (m, 1H);  $^{31}\text{P}$  NMR (162 MHz,  $\text{CDCl}_3$ ):  $\delta$  = 31.8 (dd,  $J_{\text{Pb,Pd}}$  = 474 Hz,  $J_{\text{Rh,Pb}}$  = 100 Hz), 24.3 ppm (dd,  $J_{\text{Pb,Pb}}$  = 474 Hz,  $J_{\text{Rh,Pb}}$  = 93 Hz); IR (KBr):  $\tilde{\nu}$  = 3054 (s), 2923 (s), 1695 (s), 1652 (s), 1635 (s), 1595 (s), 1482 (s), 1456 (s), 1433 (s), 1384 (s), 1325 (s), 1225 (s), 1189 (s), 1092 (s), 1044 (s), 1022 (s), 791 (s), 751  $\text{cm}^{-1}$  (s); (LIFDI):  $m/z$  calcd for  $\text{Rh}(\text{C}_{27}\text{H}_{21}\text{PO})_2$ : 887.17 [ $\text{M}]^+$ ; found: 887.16.

## Acknowledgements

We thank Professor Todd B. Marder (Institut für Anorganische Chemie, Würzburg) for his insight into the geometry of  $\text{Rh}^{\text{I}}$ -phosphine complexes. A.G.J. was funded by an EPSRC DTA PhD studentship. We thank Dr. A. Wild for part-funding SEB's PhD studentship (York Wild Fund). I.J.S.F. thanks the Royal Society for support (University Research Fellow). EPSRC grant EP/D078776/1, P.E.S., part-funded this work. We are grateful to the referees for their constructive and critical reading of our manuscript.

- [1] a) H. B. Lee, P. M. Maitlis, *J. Organomet. Chem.* **1973**, 57, C87–C89; b) J. A. Ibers, *J. Organomet. Chem.* **1974**, 73, 389–400.
- [2] S. Bernès, R. A. Toscano, A. C. Cano, O. G. Mellado, C. Alvarez-Toledano, H. Rudler, J. C. Daran, *J. Organomet. Chem.* **1995**, 498, 15–24.
- [3] a) C. Alvarez-Toledano, E. Delgado, B. Donnadieu, E. Hernandez, G. Martin, F. Zamora, *Inorg. Chim. Acta* **2003**, 351, 119–122; b) F. Ortega-Jiménez, M. C. Ortega-Alfaro, J. G. Lopez-Cortes, R. Gutierrez-Perez, R. A. Toscano, L. Velasco-Ibarra, E. Pena-Cabrera, C. Alvarez-Toledano, *Organometallics* **2000**, 19, 4127–4133; c) S. Rivo-manana, C. Mongin, G. Lavigne, *Organometallics* **1996**, 15, 1195–1207.
- [4] S. V. Osintseva, F. M. Dolgushin, N. A. Shteitser, P. V. Petrovskii, A. Z. Kreindlin, L. V. Rybin, M. Y. Antipin, *Organometallics* **2005**, 24, 2279–2288.
- [5] N. W. Alcock, P. Meester, T. J. Kemp, *J. Chem. Soc. Perkin Trans. 2* **1979**, 921–926.
- [6] A. Z. Rubezhov, *Russ. Chem. Rev.* **1988**, 57, 1194–1207.
- [7] a) M. C. Mazza, C. G. Pierpont, *J. Chem. Soc. Chem. Commun.* **1973**, 207–208; b) C. G. Pierpont, M. C. Mazza, *Inorg. Chem.* **1974**, 13, 1891–1895; c) T. Ukai, H. Kawazura, Y. Ishii, J. J. Bonnet, J. A.

- Ibers, *J. Organomet. Chem.* **1974**, *65*, 253–266; d) H. Kawazura, H. Tanaka, K. Yamada, T. Takahashi, Y. Ishii, *Bull. Chem. Soc. Jpn.* **1978**, *51*, 3466–3470.
- [8] a) I. J. S. Fairlamb, *Org. Biomol. Chem.* **2008**, *6*, 3645–3656; b) I. J. S. Fairlamb, A. F. Lee, *Organometallics* **2007**, *26*, 4087–4089; c) I. J. S. Fairlamb, A. R. Kapdi, A. F. Lee, *Org. Lett.* **2004**, *6*, 4435–4438; d) Y. Macé, A. R. Kapdi, I. J. S. Fairlamb, A. Jutand, *Organometallics* **2006**, *25*, 1795–1800; e) I. J. S. Fairlamb, A. R. Kapdi, A. F. Lee, G. P. McGlacken, F. Weissburger, A. H. M. de Vries, L. Schmieder-van de Vondervoort, *Chem. Eur. J.* **2006**, *12*, 8750–8761; f) P. Sehnaal, H. Taghzouti, I. J. S. Fairlamb, A. Jutand, A. F. Lee, A. C. Whitwood, *Organometallics* **2009**, *28*, 824–829.
- [9] F. A. Jalón, B. R. Manzano, F. Gómez-de la Torre, A. M. López-Agenjo, A. M. Rodríguez, W. Weissensteiner, T. Sturm, J. Mahía, M. Maestro, *J. Chem. Soc. Dalton Trans.* **2001**, 2417–2424.
- [10] C. G. Pierpont, R. M. Buchanan, H. H. Downs, *J. Organomet. Chem.* **1977**, *124*, 103–112.
- [11] D. B. Dell'Amico, L. Labella, F. Marchetti, J. Samaritani, *J. Organomet. Chem.* **2011**, *696*, 1349–1354.
- [12] A. G. Jarvis, A. C. Whitwood, I. J. S. Fairlamb, *Dalton Trans.* **2011**, *40*, 3695–3702.
- [13] a) Y. Zhao, H. Wang, X. Hou, Y. Hu, A. Lei, H. Zhang, L. Zhu, *J. Am. Chem. Soc.* **2006**, *128*, 15048–15049. For related ligand effects, see: b) Q. Liu, H. Duan, X. Luo, Y. Tang, G. Li, R. Huang, A. Lei, *Adv. Synth. Catal.* **2008**, *350*, 1349–1354; c) X. Luo, H. Zhang, H. Duan, Q. Liu, L. Zhu, T. Zhang, A. Lei, *Org. Lett.* **2007**, *9*, 4571–4574; d) W. Shi, Y. Luo, X. Luo, L. Chao, H. Zhang, J. Wang, A. Lei, *J. Am. Chem. Soc.* **2008**, *130*, 14713–14720; e) H. Zhang, X. Luo, K. Wongkhan, H. Duan, Q. Li, L. Zhu, J. Wang, A. S. Batsanov, J. A. K. Howard, T. B. Marder, A. Lei, *Chem. Eur. J.* **2009**, *15*, 3823–3829.
- [14] For a general review, see: a) A. G. Jarvis, I. J. S. Fairlamb, *Curr. Org. Chem.* **2011**, *15*, 3175–3196; selected references of particular note: b) S. E. Denmark, N. S. Werner, *J. Am. Chem. Soc.* **2008**, *130*, 16382–16393; c) S. E. Denmark, N. S. Werner, *J. Am. Chem. Soc.* **2010**, *132*, 3612–3620; d) L. Firmansjah, G. C. Fu, *J. Am. Chem. Soc.* **2007**, *129*, 11340–11341.
- [15] Selected references: a) Y. Canac, N. Debono, C. Lepetit, C. Duhayon, R. Chauvin, *Inorg. Chem.* **2011**, *50*, 10810–10819; b) N. J. Destefano, D. K. Johnson, R. M. Lane, L. M. Venanzi, *Helv. Chim. Acta* **1976**, *59*, 2674–2682; c) M. Sawamura, H. Hamashima, Y. Ito, *Tetrahedron: Asymmetry* **1991**, *2*, 593–596; d) R. Schuecker, K. Mereiter, F. Spindler, W. Weissensteiner, *Adv. Synth. Catal.* **2010**, *352*, 1063–1074; e) M. N. Birkholz (née Gensow), Z. Freixa, P. W. N. M. van Leeuwen, *Chem. Soc. Rev.* **2009**, *38*, 1099–1118; f) Z. Freixa, M. S. Beentjes, G. D. Batema, C. B. Dieleman, G. P. F. van Strijdonck, J. N. H. Reek, P. C. J. Kamer, J. Fraanje, K. Goubitz, P. W. N. M. van Leeuwen, *Angew. Chem.* **2003**, *115*, 1322–1325; *Angew. Chem. Int. Ed.* **2003**, *42*, 1284–1287; g) L. Poorters, D. Armspach, D. Matt, L. Toupet, S. Choua, P. Turek, *Chem. Eur. J.* **2007**, *13*, 9448–9461; h) Z. Freixa, P. W. N. M. van Leeuwen, *Coord. Chem. Rev.* **2008**, *252*, 1755–1786.
- [16] In the solid state, we did not detect appreciable phosphine oxidation over a six month period.
- [17] a) C. S. Slone, D. A. Weinburger, C. A. Mirkin, *Prog. Inorg. Chem.* **1999**, *48*, 233–350; C. A. Mirkin, *Prog. Inorg. Chem.* **1999**, *48*, 233–350; b) P. Braunstein, F. Naud, *Angew. Chem.* **2001**, *113*, 702–722; *Angew. Chem. Int. Ed.* **2001**, *40*, 680–699.
- [18] a) I. M. Al-Najjar, *Inorg. Chim. Acta* **1987**, *128*, 93–104; b) T. Niksch, H. Görls, M. Freidrich, R. Oilunkaniemi, R. Laitinen, *Eur. J. Inorg. Chem.* **2010**, *1*, 74–94; c) J. I. van der Vlugt, R. van Duren, G. D. Batema, R. den Heeten, A. Meetsma, J. Fraanje, K. Goubitz, P. C. J. Kamer, P. W. N. M. van Leeuwen, *Organometallics* **2005**, *24*, 5377–5382.
- [19] a) W. Yao, O. Eisenstein, R. H. Crabtree, *Inorg. Chim. Acta* **1997**, *254*, 105–111; b) Y. Zhang, J. C. Lewis, R. G. Bergman, J. A. Ellman, E. Oldfield, *Organometallics* **2006**, *25*, 3515–3519; c) A. Mukhopadhyay, S. Pal, *Eur. J. Inorg. Chem.* **2006**, 4879–4887. Related references: d) E. Sadat Tabei, H. Samouei, M. Rashidi, *Dalton Trans.* **2011**, *40*, 11385–11388; e) B. Singh, M. G. B. Drew, G. Kociok-Kohn, K. C. Molloy, N. Singh, *Dalton Trans.* **2011**, *40*, 623–631.
- [20] a) L. Brammer, *Dalton Trans.* **2003**, 3145–3157; b) M. Brookhart, M. L. H. Green, G. Parkin, *Proc. Natl. Acad. Sci. USA* **2007**, *104*, 6908–6914; c) T. S. Thakur, G. R. Desiraju, *J. Mol. Struct.: THEOCHEM* **2007**, *810*, 143–154; the main review of agostic interactions: M. Brookhart, M. L. H. Green, *J. Organomet. Chem.* **1983**, *250*, 395–408.
- [21] W. I. Sundquist, D. P. Bancroft, S. J. Lippard, *J. Am. Chem. Soc.* **1990**, *112*, 1590–1596.
- [22] a) T. Leininger, A. Nicklass, H. Stoll, M. Dolg, P. Schwerdtfeger, *J. Chem. Phys.* **1996**, *105*, 1052–1059; b) C. Adamo, V. Barone, *J. Chem. Phys.* **1998**, *108*, 664–675.
- [23] T. A. Peganova, A. V. Valyaeva, A. M. Kalsin, P. V. Petrovskii, A. O. Borissova, K. A. Lyssenko, N. A. Ustynuk, *Organometallics* **2009**, *28*, 3021–3028.
- [24] A. Reed, L. A. Curtiss, F. Weinhold, *Chem. Rev.* **1988**, *88*, 899–926.
- [25] K. B. Wiberg, *Tetrahedron* **1968**, *24*, 1083–1096.
- [26] a) J. Hartwig, *Organotransition Metal Chemistry: From Bonding to Catalysis*, University Science, Sausalito, **2010**; b) R. J. Cross, *Chem. Soc. Rev.* **1985**, *14*, 197–223; c) R. S. Berry, *J. Chem. Phys.* **1960**, *32*, 933–938; d) G. K. Anderson, R. J. Cross, *Chem. Soc. Rev.* **1980**, *9*, 185–215.
- [27] D. M. Norton, E. A. Mitchell, N. R. Botros, P. G. Jessop, M. C. Baird, *J. Org. Chem.* **2009**, *74*, 6674–6680.
- [28] C. Amatore, A. Jutand, G. Meyer, *Inorg. Chim. Acta* **1998**, *273*, 76–84.
- [29] D. J. M. Sneliders, C. van der Burg, M. Lutz, A. L. Spek, G. van Koten, R. J. M. K. Gebbink, *ChemCatChem* **2010**, *2*, 1425–1437.
- [30] M. L. H. Green, L.-L. Wong, A. Sella, *Organometallics* **1992**, *11*, 2660–2668.
- [31] Solvent disorder is noted in this X-ray diffraction data. Nevertheless, a reasonable structure of  $[\text{Pd}^0(\text{L})_2]$  could be determined.
- [32] W. A. Herrmann, W. R. Thiel, C. Broßmer, K. Öfele, T. Priemeier, W. Scherer, *J. Organomet. Chem.* **1993**, *461*, 51–60.
- [33] a) X. Mei, C. Wolf, *J. Org. Chem.* **2005**, *70*, 2299–2305; b) Y. Ting, Y. H. Lai, *J. Am. Chem. Soc.* **2004**, *126*, 909–914; c) E. Bosch, C. L. Barnes, N. L. Brennan, G. L. Eakins, B. E. Breyfogle, *J. Org. Chem.* **2008**, *73*, 3931–3934; N. L. Brennan, G. L. Eakins, B. E. Breyfogle, *J. Org. Chem.* **2008**, *73*, 3931–3934.
- [34] Q. Li, K. Wongkhan, X. Luo, A. Batsanov, J. A. K. Howard, Y. Lan, Y. Wu, T. B. Marder, A. Lei, *Chin. Sci. Bull.* **2010**, *55*, 2794–2798.
- [35] P. W. Clark, G. E. Hartwell, *Inorg. Chem.* **1970**, *9*, 1948–1951.
- [36] a) K. D. Tau, D. W. Meek, T. Sorrell, J. A. Ibers, *Inorg. Chem.* **1978**, *17*, 3454–3460; b) T. M. Douglas, J. Le Nôtre, S. K. Brayshaw, C. G. Frost, A. S. Weller, *Chem. Commun.* **2006**, 3408–3410.
- [37] In unpublished work we have established that a ferrocene-derived “Lei” ligand (the phenyl group is replaced by a mono-substituted ferrocene) can form a dinuclear bringing  $\text{Rh}^I$  structure. However, in that case one olefin, one carbonyl and one phosphine coordinate each  $\text{Rh}^I$  centre, which are square planar. S. E. Bajwa, Ph.D. thesis, University of York, **2012**.
- [38] We tentatively suggest that these  $\text{Rh}^I$  complexes do not behave as idealised spherical particles, thus their radii cannot be accurately determined by the Stokes–Einstein equation.
- [39] R. M. Ward, A. S. Batsanov, J. A. K. Howard, T. B. Marder, *Inorg. Chim. Acta* **2006**, *359*, 3671–3676.
- [40] C. Jiménez-Rodríguez, F. X. Roca, C. Bo, J. Benet-Buchholz, E. C. Escudero-Adán, Z. Freixa, P. W. N. M. van Leeuwen, *Dalton Trans.* **2006**, 268–278.
- [41] The aromatic protons of the major product integrates to four more than expected due to underlying protons from the minor product, which could not be independently identified.

Received: October 10, 2012  
Published online: March 11, 2013